Finite element analysis of the mechanical behavior of the different angle hip femoral stem

6 authors, including:

Murat Yaylacı
Recep Tayyip Erdoğan Üniversitesi
37 PUBLICATIONS   434 CITATIONS

SEE PROFILE

Hasan Ölmez
Karadeniz Technical University
13 PUBLICATIONS   50 CITATIONS

SEE PROFILE

Ecren Uzun Yaylaci
25 PUBLICATIONS   127 CITATIONS

SEE PROFILE

Mehmet Emin Özdemir
Çankırı Karatekin Üniversitesi
3 PUBLICATIONS   7 CITATIONS

SEE PROFILE

Some of the authors of this publication are also working on these related projects:

Project   Verification of the Artificial Neural Network Method for the Identification of Pathogenic Bacteria Causing Disease in Sea Bass (Dicentrarchus labrax) View project

Project   Polietilen Malzemeden Kültür Balıkçılığı Servis Teknesi Tasarımı View project

Finite element analysis of the mechanical behavior of the different angle hip femoral stem

Yılmaz Güvercin[1], Murat Yaylacı[*2], Hasan Ölmez[3],
Ecren Uzun Yaylacı[4], Mehmet Emin Özdemir[5] and Ayberk Dizdar[6]

[1]*Department of Orthopaed and Traumatol, Recep Tayyip Erdogan University, 53100, Rize, Turkey*
[2]*Department of Civil Engineering, Recep Tayyip Erdogan University, 53100, Rize, Turkey*
[3]*Department of Marine Engineering Operations, Karadeniz Technical University, 61530, Trabzon, Turkey*
[4]*Surmene Faculty of Marine Science, Karadeniz Technical University, 61530, Trabzon, Turkey*
[5]*Department of Civil Engineering, Cankiri Karatekin University, 18100, Çankırı, Turkey*
[6]*Department of Biomedical Engineering, Kocaeli University, 41380, Kocaeli, Turkey*

Abstract. Femoral stems with proximal metaphyseal involvement are commonly used total hip replacement components with very good results. In this study, total hip arthroplasty (THA) application was analyzed using a three-dimensionally modeled human hip joint by finite element method. The aim of the study is to investigate the effects of changes in the direction of the femoral stem on these complications. Finite element analysis is performed on a model of femur bone by varying the femur angles. Finite element models were prepared for three different positions (5 degrees varus, neutral, 5 degrees valgus) on the femur without cement during walking motions. A sinusoid dynamic load with amplitude between 300 N and 1700 N and with a frequency of 1 Hz was applied. The stresses, strains and deformations that occurred on the femur and stems were determined at the end of the finite element analysis and compared to each other. Considering the results of strain, strain and deformation in the study, it is seen that the closest results to the natural load bearing of the femur are in the valgus position. The results obtained in the neutral position are also close to these results. In the metaphyseal points involving the femur stem, the highest values were found in the varus position. In all three positions, the femoral stem provides the transfer of the load from the proximal femur. The lowest stress, strain and deformation results were obtained in the valgus position, especially in the metaphyseal where the prosthesis is involved. It is seen that there are values close to this in the neutral position. This situation may be thought to result in a decrease in the proximal stress shield, an increase in bone protection compared to the varus position, a long-term loosening and a decrease in periprosthetic fracture.

Keywords: biomechanics; finite element method; total hip arthroplasty

1. Introduction

Total hip arthroplasty (THA) is a successful method that frequently used for long-term pain relief and restoration of function for patients with diseased or damaged hips (Reimeringer and Nuño 2016). Aseptic loosening, bone resorption, pain, post-prosthetic bone fractures, and dislocations are the

---

∗Corresponding author, Associate Professor, E-mail: murat.yaylaci@erdogan.edu.tr

main causes of this restoration (Talip and Kişioğlu 2019). The total number of hip arthroplasties performed increases every year. The increase in the number of operations causes an increase in the failure rate. The long-time performance of this operation is bound up with a diversity of factors, such as the surgical method used, the placing of the stem, the stability of the intramedullary fixation, the patient weight, and the stem design. Before clinical application, the effects of prostheses used in THA on the patient in terms of mechanical behavior should be determined. Before the clinical use of the prostheses used in THA, the stresses, deformations and displacements that will occur in the bone can be calculated by using the finite element method.

Many solution methods are used in solving mechanical problems (Keshtegar *et al.* 2020, Kolahchi *et al.* 2020, Azizkhani *et al.* 2020, Shariati *et al.* 2021, Huang *et al.* 2021, Al-Furjan *et al.* 2020, 2021a, b, Kolahchi *et al.* 2021, Hajmohammad *et al.* 2021, Motezaker *et al.* 2021). Based on the evolution of today's computers, numerical analysis acquires an important role in the biomechanical investigation (Cheruvu *et al.* 2016, Tomlin *et al.* 2016). General practice in numerical analysis is the finite element method (FEM), which can be applied in different situations, e.g., in structure mechanics, thermodynamics or biomechanics (Shariati *et al.* 2020, Al-Furjan *et al.* 2020a, b, 2022, Keshtegar *et al.* 2021, Kolahchi and Kolahdouzan 2021, Taherifar *et al.* 2021). Structural mechanical point of view deals with deformation, stress and strain analysis of bone and stem. For this reason, FEM is widely used in biomechanics to analyze mechanical behavior and to answer unresolved questions related to clinical complications.

The literature includes articles on analyzing the mechanical behavior of the femur bone by using FEM (Hambli 2014, El Sallah *et al.* 2020, Mobasseri *et al.* 2020, Ramakrishna and Pavani 2020). Watanabe *et al.* (2000) evaluated the stress concentration and stress shielding after hip arthroplasty using three dimensional finite element models. FEM was used to analyze stress distribution during normal walking, standing up, stair climbing and knee-bend boundary conditions by Pastrava *et al.* (2009) and Michalski *et al.* (2017). Li *et al.* (2014) evaluated the fracture process in the cortical bone at a micro-scale using FEM. Kumar *et al.* (2015) handled three dimensional femur bone using FEM and the bone was analyzed for hip contact stresses and forces during walking, standing, running and jumping activities. Stress, strain, determination and fracture on bone were studied by using FEM by Parashar and Sharma (2016). Reimeringer and Nuno (2016) examined the effect of the contact ratio and its location on the primary stability of a cementless stem subjected to stair climbing using finite element analysis. Wang *et al.* (2017) examined the contact areas and pressures between the femoral head and the acetabulum during walking using FEM. Abdullah *et al.* (2017) analyzed the effects of different types of femoral components, namely total hip arthroplasty and resurfacing hip arthroplasty, on predicting the risk of femoral fractures using FEM. Kalaiyarasan *et al.* (2020) studied on investigated improving the strength of bone joints made up of dissimilar biomaterials and tried to find out the best material by using FEM. Wadatkar *et al.* (2020) investigated the effect of biomaterials used for an implant on stress analysis and fracture in a human body with the help of FEM. Biomechanical studies have been conducted by researchers in different fields of medical sciences using the finite element method Nişanci *et al.* (2020), Terzi *et al.* (2020).

Loosening, osteolysis and periprosthetic fracture are seen as of late complications after total hip arthroplasty. The aim of this study is to investigate the effects of changes in the direction of the femoral stem on these complications. For this reason, we analyzed the change in stress, strain and determination of mechanical properties using software based on the finite element method by placing the stem in different positions (5 degrees varus, neutral, 5 degrees valgus) on the femur without cement. The mechanical effects of the incorrectly placed stem on the bone were evaluated. We compared stem placed at different angles by measuring stress, strain and deformation. As far as
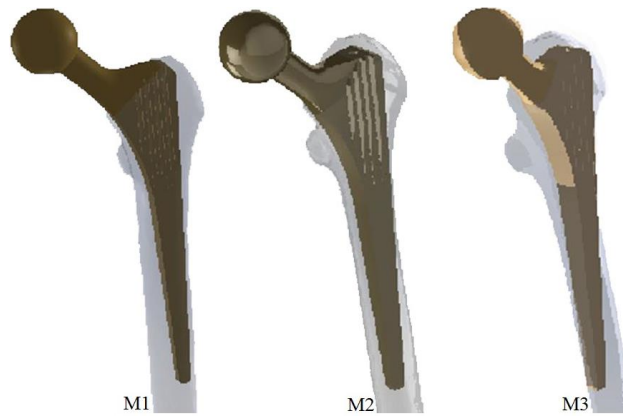
Fig. 1 Stem angles, (M1-5° (varus), M2-neutral, M3-5° (valgus))

we know, there is no FEM study in the literature that examines the placement angle of the femoral stem in as much detail as this study. The results obtained will contribute to the application of the most appropriate THA stem placement with the help of a computer without performing any operation on the patient before surgery (THA).

2. Definition of the problem

Femur bone is known as the longest and strongest bone in the human body. The length of this bone is about 26% of the height of a human being. The upper part consists of head, neck and two trochanters. The cylindrical body is the long part of the femur. The slightly cuboid (diagonal diameter is bigger than its anteroposterior) lower part is bigger than the upper one.

For the biomechanical analyses, we selected the CLS Spotorno stem (Zimmer, Warsaw, USA), clinically and biomechanically well established as cementless THA stem (Aldinger *et al.* 2009, Schmidutz *et al.* 2017).

In order to determine the effect of implant placement, we analyzed it with 3 different stem angles in the femoral shaft: Model 1 (M1) 5° (varus), Model 2 (M2) neutral and Model 3 (M3) 5° (valgus) (Fig. 1).

3. Materials and method

The analyzed structures in biomechanics are man-made and have a biological origin. When the femur is analyzed, there are no exactly defined angles, curves and distances. The femur has the ability to adapt to any situation mechanically. Especially with regard to implant technology and arthroplasty, it plays an important role in orthopaedic biomechanics. If the operation and the design of the stem are wrong, the distribution of the stress around the treated joint occurs improperly. If the forces are mainly transferred by the stem, femur and stem contact regions get minimally loaded. This is another problem that can be solved by stress, strain, and deformation analysis of the stem-femur compound. These models are subjected to transient structural analysis using ANSYS Workbench to evaluate the stress, strain, and deformation.
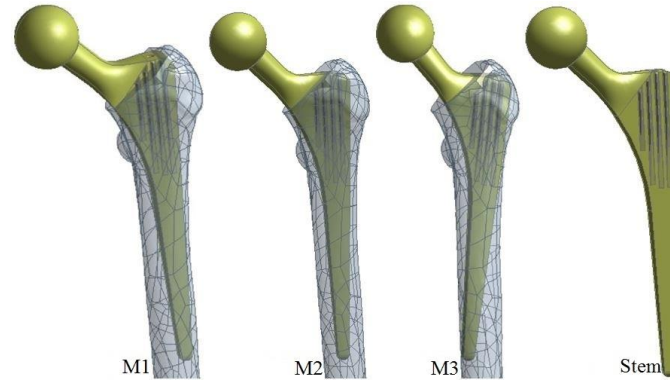
Fig. 2 Geometry for models (M1, M2, M3, Stem)

3.1 Modeling

In the last twenty years with dramatic development in efficiently modeling, analyzing and designing complex structures, FEM has become the most widely used numerical method such as industrial structures, machines and human organs. The FEM was applied first in biomechanical orthopedics to investigate the stress in human bones (Brekelmans *et al.* 1972). To this end, FEM helps to predict biomechanical behaviors of biological tissues at a particular location in complex systems both in living organism and in laboratory.

The stem and femur to be analyzed in the FEM can be designed using CAD-software. Although there are many methods to model a femur bone of which computer tomography scan and MRI data due to unavailability of such data, virtual femur bone and stems models were designed and assembled in the SolidWorks program as in the real medical operations (SolidWorks 2018). For 3D solid models of THA modeling, bone and stem parts were prepared and assembled. Then, the models were transferred to the ANSYS Workbench software for transient structural analysis (Fig. 2) (ANSYS 2016). Dimensions of CLS stem (for Head M) are used for size 11.25 (Zimmer). The models were created with an addiction angle of 16° in the frontal plane and 9° flexion angle in the sagittal plane for the loading conditions (Bergmann *et al.* 2001).

Three dimensional finite element models of both models were automatically generated with 5-node tetrahedron elements (tetrahedron elements with four nodes). SOLID 187 tetrahedron element was used for the finite element models. The contact type between bone and stem was defined as CONTA 172 and TARGE 169 elements. We applied the transient structural type of analysis, which allows time dependent loading.

3.2 Material properties

Material properties of the femur are different between humans so that it does not assign any certain material properties. The bone material is anisotropic in nature, but the material properties of all models were assumed to be linear, elastic, and isotropic. The reason is that a small part of the bone can be solved for an anisotropic solution however for complete bone; it is extremely difficult to assign anisotropic material properties. The material properties of all models were assumed to be linear, elastic, and isotropic. The only cortical part was modeled in this study (Anwar *et al.* 2017, Peleg *et al.* 2006). Each element must be assigned to the appropriate elastic constants of the material

Table 1 The material properties of the models

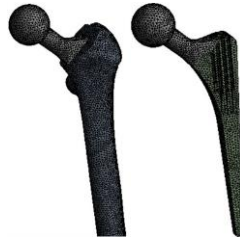|	Materials	Density (g/cm^3)	Modulus of elasticity (*MPa*)	Poisson's ratio
Stem	Ti6Al4V	4.43	113800	0.34
Femur	Bone	2.1	17000	0.35

Fig. 3 Finite element meshes of the model

in the finite element model. Three material constants (elastic modulus, Poisson's ratio, and density) were required. The material properties of Titanium Alloy (Ti6Al4V), the most used for the prosthesis were described for the prostheses (Wadatkar *et al.* 2020). The CLS Spotorno type of femoral stem was modeled for this study. The material properties of the femur bone were defined according to the study of Tu *et al.* (2009). The properties of the material used for the model are represented in Table 1.

3.3 Loading and boundary conditions

The application of boundary conditions and loading in biomechanical FEM is based on suppositions including forces acting in the human body, displacements and symmetry boundary conditions based on simplifications in the model. The major source of acting loads in the musculoskeletal system for orthopedic biomechanics is the telemetric in vivo measurement using instrumented stems (Bergmann *et al.* 1993, 2001).

In this study, different configurations were evaluated to emphasize the effects of various assembling conditions of bone and stem. The boundary condition was applied by fixing the distal epiphysis, which is the lower part of the femur that is connected to the knee. For the loading conditions, the samples were dynamically loaded under physiological adapted conditions according to in vivo measurements obtained for a person with a bodyweight of 70 kg, walking on ground level. A sinusoid dynamic load with amplitude between 300 N and 1700 N and with a frequency of 1 Hz was applied for 30 cycles per analysis (Fottner *et al.* 2009). The load was applied to the head of the model.

3.4 Meshing

A mesh convergence study was performed by refining the element size from 5 mm to 2 mm. Changing mesh sizes had different results in terms of stresses. Stresses change significantly when mesh size decreases from the initial 5 mm size to 2 mm. Beyond the mesh size lesser than 2 mm, there are no significant changes in stresses for subsequent mesh size. Thus, the most convenient element size for the optimum results was defined as 2 mm for the analysis of all the models. A femur and stem THA model consisting of 134894 nodes and 87061 elements is shown in Fig. 3.
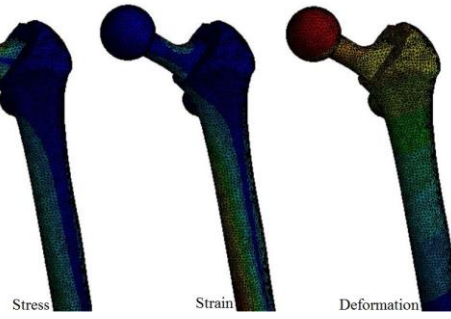
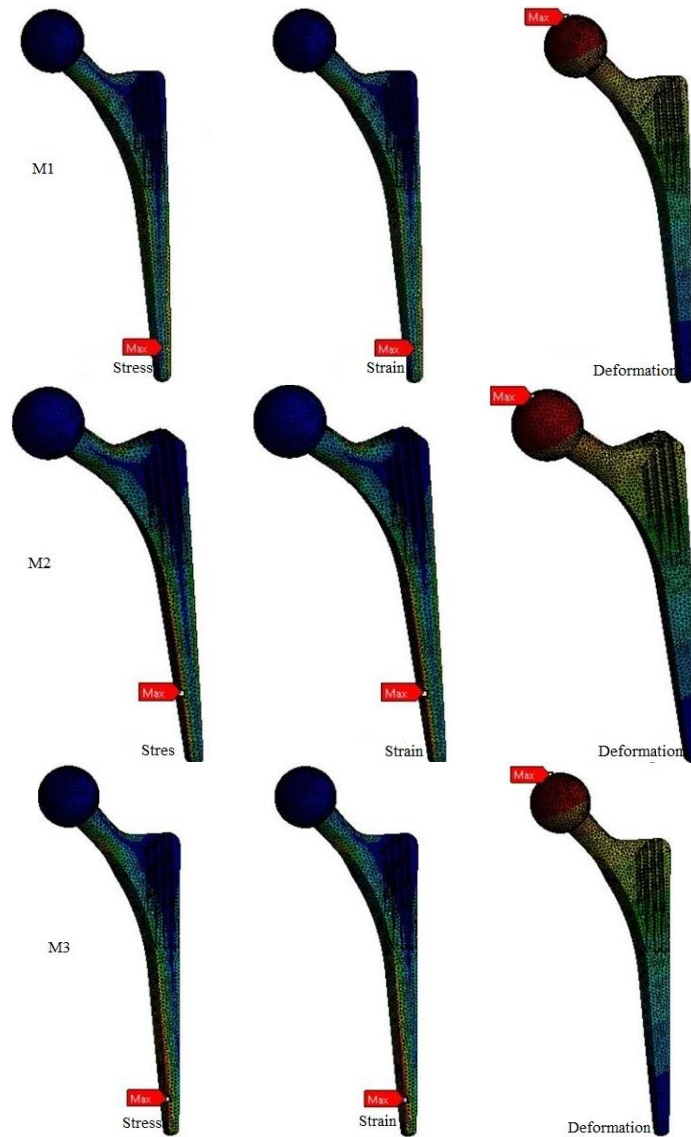*Yılmaz Güvercin et al.*

Fig. 4 Stress, strain, deformation

Fig. 5 Results of the maximum stress, strain, and deformation in the stem

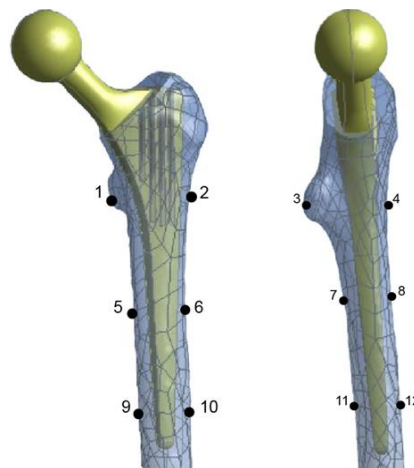Fig. 6 Results of the maximum stress, strain, and deformation in the femur

Fig. 7 Positions of points

3.5 Solve

In order to evaluate the influence of the stem angles, three finite element models of the stem-femur compound were generated. The structural response of the stem-bone compound to the applied forces was calculated using the transient structural analysis ANSYS Workbench (Fig. 4).

Table 2 Results of the maximum stress, strain, and deformation in the stem

Models	Max. Von-Mises Stress (MPa)	Max. Strain (10^{-4})	Max. Deformation (mm) (10^{-4})
M1	98.568	8.6616	6.4534
M2	85.091	7.4774	5.9353
M3	80.386	7.0034	4.7509

Table 3 Results of the maximum stress, strain, and deformation in the femur

Models	Max. Von-Mises Stress (MPa)	Max. Strain (10^{-4})	Max. Deformation (mm)
M1	42.833	0.25203	5.1066
M2	38.252	0.22516	4.7289
M3	31.955	0.19973	3.7622

Table 4 Results of the stress at points in the stem (MPa)

Models	1	2	3	4
M1	36.431	30.054	6.3522	6.8412
M2	32.211	27.539	5.9103	4.5044
M3	27.219	25.811	4.6719	2.1517
	5	6	7	8
M1	59.988	84.400	28.261	18.901
M2	51.166	68.298	18.501	16.717
M3	43.462	59.455	11.587	14.476
	9	10	11	12
M1	78.225	50.962	73.550	38.185
M2	71.207	37.425	68.529	18.624
M3	60.282	21.582	56.409	16.923

Table 5 Results of the stress at points in the femur (MPa)

Models	1	2	3	4
M1	12.34	9.0005	2.7433	1.5699
M2	10.884	6.2813	1.2595	1.1163
M3	9.7017	5.2473	0.5692	0.84165
	5	6	7	8
M1	29.311	19.029	2.6522	9.994
M2	24.525	17.747	1.9015	6.6048
M3	16.496	13.580	1.4848	3.8039
	9	10	11	12
M1	31.977	17.958	9.6771	11.330
M2	28.480	15.677	8.4626	8.1644
M3	13.736	11.566	7.9950	6.4488

4. Numerical results

In this study, the finite element method was used to obtain stress, strain, and deformation values in each region of the femur and stem. Titanium was used as a stem material for all models. The

Table 6 Results of the strain at points in the stem (10^{-4})

Models	1	2	3	4
M1	3.1678	2.6156	4.4356	6.1540
M2	2.9970	2.2847	3.3506	5.5784
M3	2.4024	2.1663	2.3831	4.6886
	5	6	7	8
M1	5.2363	7.4065	2.4922	1.706
M2	4.2627	6.0010	1.4165	1.4288
M3	3.8130	5.2218	1.0190	1.2624
	9	10	11	12
M1	7.4913	7.3535	6.9406	2.1520
M2	6.1415	3.3126	5.7558	1.6891
M3	5.0347	1.0542	5.3686	1.4896

stress, strain, and deformation images and numerical values of the analysis results for the Model 1 (M1), Model 2 (M2), and Model 3 (M3) are shown in Figs. 8-10 and in Tables 2-5, respectively.

The stress, strain, and deformation images and numerical values of the analysis results for the stem and femur are shown in Figs. 5-6 and in Tables 2-3, respectively. As can be seen from the tables, the highest stress, strain, and deformation values were obtained in the M1. The lowest stress, strain, and deformation values were obtained in the M3.

The proximal registration points 1 and 2 were set at the level of the lesser trochanter. For both groups, the distal points 5 and 6 were positioned 1.5 cm above the tip of the stem. Measurement points 3 and 4 were located centrally between the proximal and distal levels (Fottner *et al.* 2009). On the three different stem-femur compound designs twelve points were measured for each model. The stress, strain, and deformation values obtained are shown in Tables 4-9.

When the numerical data in Tables 4-9 are examined, it is seen that the results obtained using M1, M2, and M3 designs were different from each other. In terms of models, the maximum values were obtained when using M1, while the lowest values were obtained in M3.

When Table 4 and Table 5 are considered in terms of points, it is seen that the highest three stress values for stem and femur are determined at points M1-6, M1-9, M1-11 and M1-5, M1-9, M2-9, respectively. On the other hand, the lowest three stress values for stem and femur are determined at points M3-4, M2-4, M3-3 and M3-3, M3-4, M2-4, respectively. Considering the stress values for the stem and femur at the points shown in Fig. 7, it is seen that the stresses increase in (1-5-9), (3-7-11) and (4-8-12) directions. When passing from point 2 to point 6, the stress value increases but decreases at the transition from 6 to 10.

When Tables 6-7 are considered in terms of points, it is seen that the highest three strain values for stem and femur are determined at points M1-4, M1-2, M1-3 and M1-1, M1-4, M1-3, respectively. On the other side, the lowest three strain values for stem and femur are determined at points M3-7, M3-10, M3-8 and M3-7, M2-7, M3-8, respectively. When Tables 6 and 7 are examined, strains in the direction of the points (1-5-9) increase both in the stem and in the femur. The strain value increases when moving from point 2 to point 6, but decreases from point 6 to point 10. The strain decreases in the direction of 3 to 7 point, and increases in the direction of 7 to 11. The same is true towards the (4-8-12) points. The strains decrease in the 4-8 direction and increase in the 8-12 direction.

Table 7 Results of the strain at points in the femur (10^{-4})

Models	1	2	3	4
M1	7.2695	5.5235	5.1583	7.4062
M2	6.4472	3.9729	4.0974	6.8730
M3	5.6737	3.3587	3.4048	5.8392
	5	6	7	8
M1	17.244	11.192	1.5633	5.8784
M2	14.360	10.044	1.2298	3.8587
M3	9.7044	7.9912	1.0813	2.2380
	9	10	11	12
M1	18.812	10.567	5.6881	6.6555
M2	16.758	8.2785	5.0476	4.7973
M3	8.078	6.8522	9.9427	3.7180

Table 8 Results of the deformation at points in the stem (mm)

Models	1	2	3	4
M1	3.7769	3.7928	3.7781	3.8310
M2	3.4314	3.4273	3.3985	3.4418
M3	2.7515	2.6518	2.6639	2.7221
	5	6	7	8
M1	2.3125	2.3675	2.298	2.3908
M2	2.1693	2.1494	2.1445	2.1695
M3	1.7828	1.6834	1.7439	1.7156
	9	10	11	12
M1	1.1354	1.17830	1.1603	1.1335
M2	0.93292	0.92665	0.94529	0.92395
M3	0.84694	0.83918	0.85324	0.87478

Table 9 Results of the deformation at points in the femur (mm)

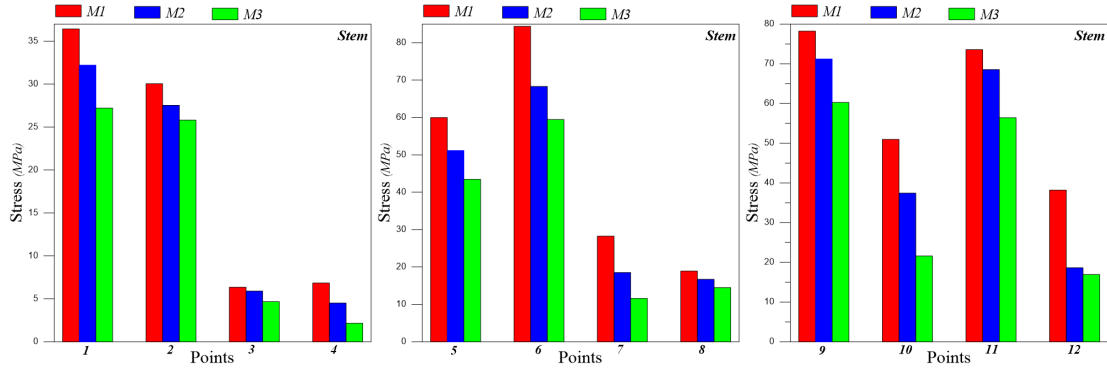| Models	1	2	3	4
M1	3.6132	3.5618	3.5913	3.6051
M2	3.3464	3.3649	3.3266	3.3356
M3	2.6997	2.6433	2.6862	2.6435
	5	6	7	8
M1	2.3713	2.4265	2.3277	2.4881
M2	2.2241	2.1921	2.1594	2.262
M3	1.9147	1.6954	1.8296	1.7828
	9	10	11	12
M1	1.3685	1.1794	1.1400	1.0864
M2	0.98583	0.98583	0.9446	0.94607
M3	0.8535	0.73028	0.86817	0.86525

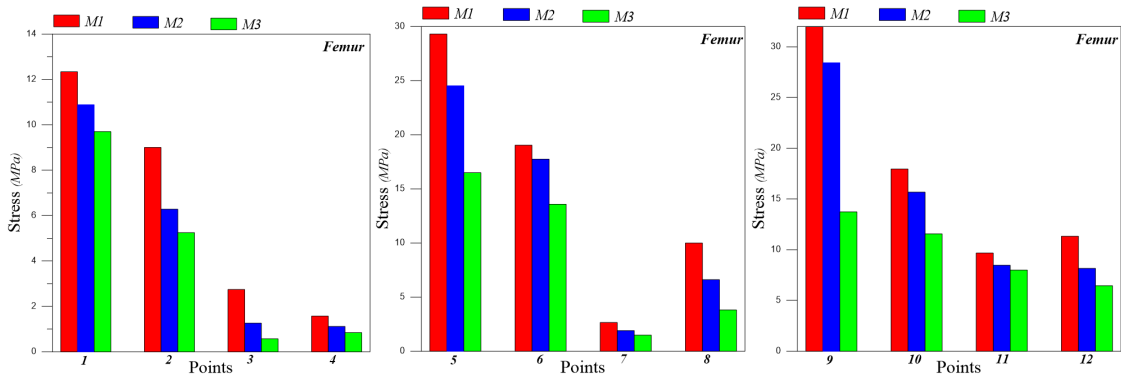Fig. 8 Stress at points in the stem

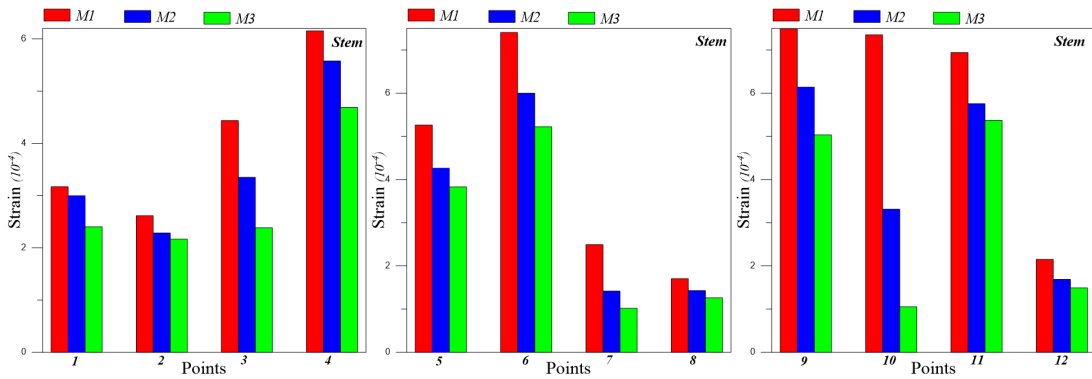Fig. 9 Stress at points in the femur

Fig. 10 Strain at points in the stem

When Tables 8-9 are considered in terms of points, it is seen that the highest three deformation values for stem and femur are determined at points M1-6, M1-9, M1-10 and M1-5, M1-9, M2-9, respectively. On the other hand, the lowest three deformation values for stem and femur are determined at points M3-10, M3-9, M3-11 and M3-10, M3-9, M3-12, respectively. When the deformation values obtained are considered, the deformation in the direction of (1-5-9), (2-6-10), (3-7-11), and (4-8-12) points decreases both in the stem and in the femur.
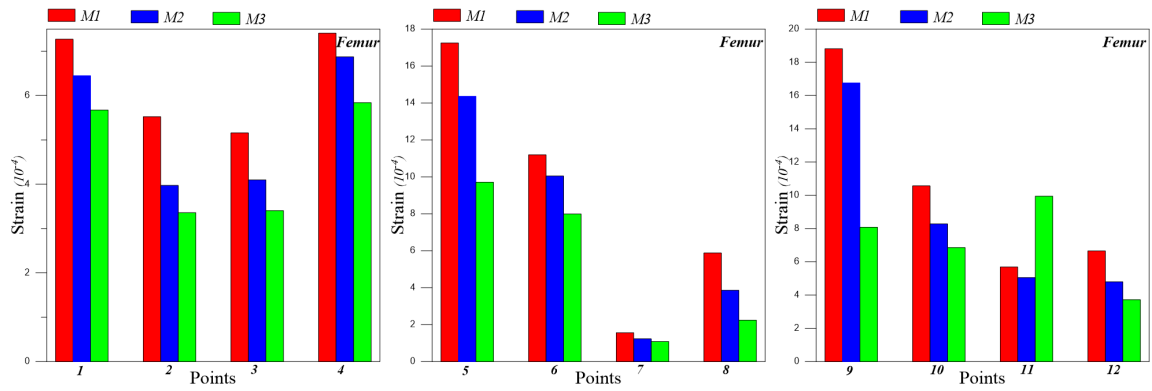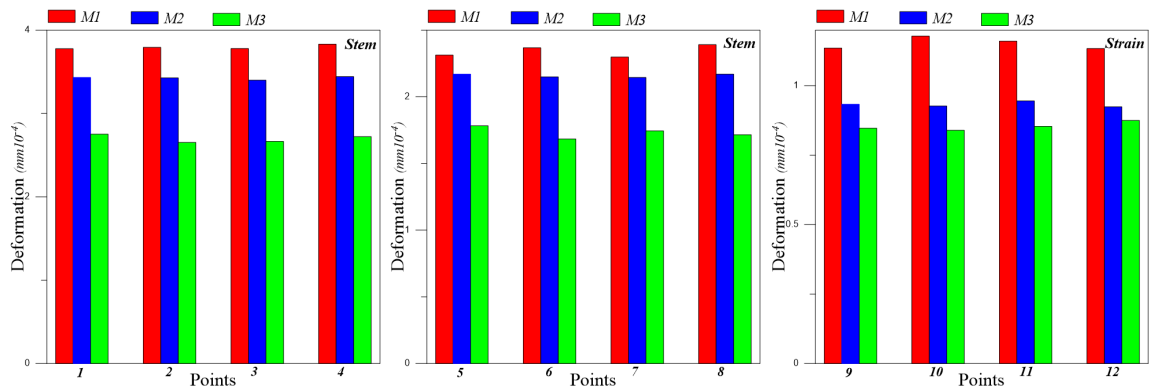
Fig. 11 Strain at points in the femur

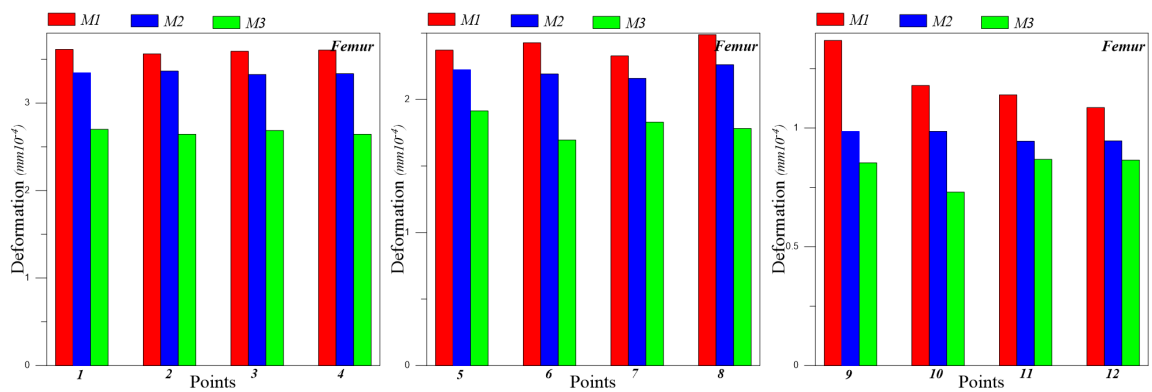Fig. 12 Deformation at points in the stem

Fig. 13 Deformation at points in the femur

5. Discussion

Nowadays, THA is an effective treatment of osteoarthritis on the hip due to various reasons and its results are very good. However, in cementless THA applications, unsuccessful results occur in patients in the short and long terms. The long-term failure rate is reported to be 10% (Bordini *et al.*

2007). This failure depends on factors such as surgery, patient characteristics, and prosthesis type. The main purpose of this study is to minimize these unsuccessful results. For this reason, the stem placement at different angles in the femoral stem model, which is widely used and has metaphyseal involvement was evaluated mechanically. 3D femoral stem layer model was created and analyzes were made with the help of a package program based on the finite element method. As a result of the analysis, the deformation, strain and stresses in the femur and the stem were obtained and presented in tables and graphics. This numerical study examined the stem angle in the femur from a biomechanical perspective for use in clinical applications. When the numerical results obtained are examined, it is seen that the lowest stress, strain, and deformation values in the femur and stem under dynamic load are in the valgus position (M3). The values obtained in the neutral position (M2) are between the values obtained from the valgus and varus positions and are closer to the valgus position. On the contrary, in the varus position (M1), the values were found to be very high and open to clinical complications (Figs. 8-13).

THA is the most effective treatment for calcification of the hip due to various reasons. The design, material and application of the prosthesis used are the main factors affecting the success. Success can be measured by properly transmitting the body load to the thigh. Load transfer in long bones normally occurs with subchondral bones. In prosthetic patients, load transfer is provided by the attachment of the stem to the femur from various regions (Cristofolini 2017). It has been reported that prostheses with metaphyseal involvement rather than diaphyseal involvement have better results (Gardner *et al.* 2010). In our study, a conical prosthesis with metaphyseal involvement was used. In our study, a decrease was found in the proximal femur cortex and proximal stem (1,2,3,4 points) stresses compared to other points (Yan *et al.* 2020, Bieger *et al.* 2012, Yan *et al.* 2018). It is observed that the values in the proximal femur and proximal stem are low in the strain as well as in stretching in all three implantation forms. On the other hand, deformation was found to be high in all three implantations. In this case, it can be predicted that the proximal femur stress and strain change is low and the displacement is high may cause periprosthetic bone loss (Engh *et al.* 2003).

In this study, it is seen that the deformation decreases and the stress and strain increase as towards the distal. This situation is consistent with the studies in the literature examining the stress, strain and deformation values at some points in the stem and femur (Floerkemeier *et al.* 2017, Aamodt *et al.* 2001, Yan *et al.* 2020). Unlike the general situation, stress and strain decrease at 6-10 points corresponding to the anterior of the proximal diaphysis. This could be due to the low load effect on the region caused by the stem design.

The incidence of periprosthetic femur fractures after CAP with CLS prosthesis was as low as 8 years and was reported to be 4.5% after 17 years. The authors reported that the stem placement angle did not differ in fracture incidence (Streit *et al.* 2011). In another study involving 26-32 years of follow-up after CAP with CLS prosthesis, the authors reported that more research is needed to evaluate the causes and risk factors of periprosthetic fractures (Peitgen *et al.* 2019). The popularity of direct anterior prosthesis application is increasing day by day, and varus placement is widely seen in studies. It has been reported that varus localization of the femoral stem may have adverse effects on patients (Haversath *et al.* 2020, Zang *et al.* 2018). Although it was stated in long-term studies with CLS prosthesis that the femoral stem placement angle would not affect the life of the prosthesis, in a study with a wide participation, the authors reported that the risk of periprosthetic fracture might increase in the positioning of valgus above 3 degrees and varus above 5 degrees (Griffiths *et al.* 2020).

When the implantation types of varus, valgus and neutral were evaluated among themselves, the stress, strain and displacement values in the proximal femur were highest in the varus position and
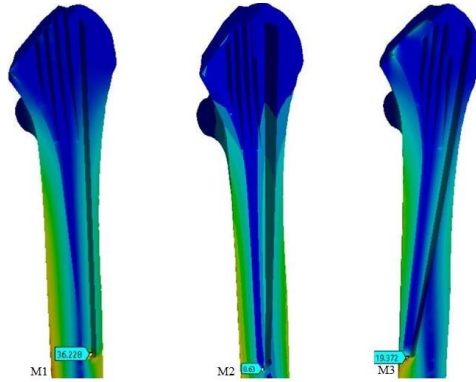
Fig. 14 Stress distributions in the three FE models

the lowest in the valgus position. When the femur diaphysis area was examined, it was observed that it was the lowest in the valgus position and the highest in the varus position, as in the proximal region. Considering the endpoint of the distal stem, it is seen that the lowest stress value is in the neutral position and the highest value is in the varus position (Fig. 14). Fig. 14 is an internal cross-sectional view of the femur without the stem. The increase in stress will cause an increase in the fibrous tissue that will disrupt the osseointegration at the bone implant border and will cause cracks in the bone or stem. It would be the right approach to think that this situation will increase the risk of periprosthetic fractures by tiring the bone or stem in the long term. These stresses will cause deformations in the bone, especially in the valgus, and varus positions. These deformations are thought to cause bone fractures over time.

There are many cemented prosthesis studies on incorrect femoral stem positioning. On the contrary, there are few studies done with cementless prostheses. In THA applications, % 46 percent of femoral stem placements are at least one degree of varus or valgus position. Six of these patients had cortical hypertrophy and nine of them had proximal region osteolysis (Shishido *et al.* 2018). In this study, especially the mechanical effects of cementless prosthesis placement are examined and the literature on the subject is contributed.

6. Conclusions

The aim of this study is to measure the stress, strain, and deformation created by the femoral stem placed in different positions under dynamic load. Accordingly, the damages that may occur in the femur and stem were evaluated in accordance with the clinic.

Finite element modeling is a powerful method in biomechanical analysis, but it has some limitations. The most important limitation in the application of FEM for biomechanics is the lack of anatomical detail in the modeling. With the advances in computer tomography, some of these limitations have been solved. When the parameters required for the design are known the results from FEM can be utilized effectively for stem design and application.

As a conclusion, this study compared stress, strain, and deformation values that occurred in the cementless THA for three different stem angles. The stress, strain and deformation distributions caused by replacing the stem in the femur were analyzed with the help of the ANSYS Workbench finite element program. The results obtained are described below.

• For clinical practice, the results of the current study showed that the different angle variations of the stem in the femur have an influence on mechanical behaviors.
• With the development of computers, the accuracy of stem-femur analysis made with the finite element method has increased.
• The effects of femoral stem placement on the patient are discussed in the literature. In this study, although the mechanical values are more appropriate in the valgus position, the lowest stress values were obtained in the neutral position at the point where the distal part of the femoral stem touches the bone.

References

Aamodt, A., Lund-Larsen, J., Eine, J., Andersen, E., Benum, P. and Husby, O.S. (2001), "Changes in proximal femoral strain after insertion of uncemented femoral stems", *J. Bone Joint Surg. Am.*, **83**(6), 921-929. https://doi.org/10.1302/0301-620X.83B6.0830921.

Abdullah, A.H., Todo, M. and Nakashima, Y. (2017), "Prediction of damage formation in hip arthroplasties by finite element analysis using computed tomography images", *Med. Eng. Phys.*, **44**, 8-15. https://doi.org/10.1016/j.medengphy.2017.03.006.

Al-Furjan, M.S.H., Ali hatami, Habibi, M., Shan, L. and Tounsi, A. (2021), "On the vibrations of the imperfect sandwich higher-order disk with a lactic core using generalize differential quadrature method", *Compos. Struct.*, **257**, 113-150. https://doi.org/10.1016/j.compstruct.2020.113150.

Al-Furjan, M.S.H., Habibi, M., Ghabussi, A., Safarpour, H., Safarpour, M. and Tounsi, A. (2021), "Non-polynomial framework for stress and strain response of the FG-GPLRC disk using three-dimensional refined higher-order theory", *Eng. Struct.*, **228**, 111496. https://doi.org/10.1016/j.engstruct.2020.111496.

Al-Furjan, M.S.H., Habibi, M., Jung, D.W., Sadeghi, S., Safarpour, H., Tounsi, A. and Chen, G. (2020), "A computational framework for propagated waves in a sandwich doubly curved nanocomposite panel", *Eng. Comput.*, 1-18. https://doi.org/10.1007/s00366-020-01130-8.

Al-Furjan, M.S.H., Habibi, M., Ni, J. and Tounsi, A. (2020), "Frequency simulation of viscoelastic multi-phase reinforced fully symmetric systems", *Eng. Comput.*, 1-17. https://doi.org/10.1007/s00366-020-01200-x.

Al-Furjan, M.S.H., Habibi, M., Rahimi, A., Chen, G., Safarpour, H., Safarpour, M. and Tounsi, A. (2020), "Chaotic simulation of the multi-phase reinforced thermo-elastic disk using GDQM", *Eng. Comput.*, 1-24. https://doi.org/10.1007/s00366-020-01144-2.

Al-Furjan, M.S.H., Safarpour, H., Habibi, M., Safarpour, M. and Tounsi, A. (2022), "A comprehensive computational approach for nonlinear thermal instability of the electrically FG-GPLRC disk based on GDQ method", *Eng. Comput.*, **38**, 801-818. https://doi.org/10.1007/s00366-020-01088-7.

Aldinger, P.R., Jung, A.W., Breusch, S.J., Ewerbeck, V. and Parsch, D. (2009), "Survival of the cementless Spotorno stem in the second decade", *Clinical Orthopaedics Related Res.*, **467**(9), 2297-2304. https://doi.org/10.1007/s11999-009-0906-7.

ANSYS 16.0 (2016), Swanson Analysis Systems Inc., Houston PA, USA.

Anwar, A., Lv, D., Zhao, Z., Zhang, Z., Lu, M., Nazir, M.U. and Qasim, W. (2017), "Finite element analysis of the three different posterior malleolus fixation strategies in relation to different fracture sizes", *Injury Int. J. Care Injured*, **48**(4), 825-832. https://doi.org/10.1016/j.injury.2017.02.012.

Azizkhani, M., Kadkhodapour, J., Anaraki, A.P., Hadavand, B.S. and Kolahchi, R. (2020), "Study of body movement monitoring utilizing nano-composite strain sensors contaning carbon nanotubes and silicone rubber", *Steel Compos. Struct.*, **35**(6), 779-788. https://doi.org/10.12989/scs.2020.35.6.779.

Bergmann, G., Deuretzbacher, G., Heller, M., Graichen, F., Rohlmann, A., Strauss, J. and Duda, G.N. (2001), "Hip contact forces and gait patterns from routine activities", *J. Biomech.*, **34**(7), 859-871. https://doi.org/10.1016/S0021-9290(01)00040-9.

Bergmann, G., Graichen, F. and Rohlmann, A. (1993), "Hip joint loading during walking and running measured in two patients", *J. Biomech.*, **26**(8), 969-990. https://doi.org/10.1016/0021-9290(93)90058-M.

Bieger, R., Ignatius, A., Decking, R., Claes, L., Reichel, H. and Durselen, L. (2012), "Primary stability and strain distribution of cementless hip stems as a function of implant design", *Clin. Biomech.*, **27**(2), 158-164. https://doi.org/10.1016/j.clinbiomech.2011.08.004.

Bordini, B., Stea, S., De Clerico, M., Strazzari, S., Sasdelli, A. and Toni, A. (2007), "Factors affecting aseptic loosening of 4750 total hip arthroplasties: Multivariate survival analysis", *BMC Musculoskelet Disord.*, **8**, 69. https://doi.org10.1186/1471-2474-8-69.

Brekelmans, W.A.M., Poort, H.W. and Slooff, T.J. (1972), "A new method to analyze the mechanical behavior of skeletal parts", *Acta Orthop. Scandinav*, **43**(5), 301-317. https://doi.org/10.3109/17453677208998949.

Cheruvu, B., Tsatalis, J., Laughlin, R. and Goswami, T. (2016), "Methods to determine the volume of infrapatellar fat pad as an indicator of anterior cruciate ligament tear", *Biomater. Biomec. Bioeng.*, **3**(1), 27-35. http://doi.org/10.12989/bme.2016.3.1.027.

Cristofolini, L. (2017), "Critical examination of stress shielding evaluation of hip prostheses", *Critical Rev. Biomed. Eng.*, **45**(1-6), 549-623. https://doi.org/10.1615/critrevbiomedeng.v45.i1-6.190.

El-Sallah, Z.M., Ali, B. and Abderahmen S. (2020), "Effect of force during stumbling of the femur fracture with a different ce-mented total hip prosthesis", *Biomater. Biomec. Bioeng.*, **5**(1), 11-23. https://doi.org/10.12989/bme.2020.5.1.011.

Engh, C.A., Young, A.M., Engh, C.A. and Hopper, R.H. (2003), "Clinical consequences of stress shielding after porous-coated total hip arthroplasty", *Clinical Orthopaedics Related Res.*, **417**, 157-163. https://doi.org/10.1097/01.blo.0000096825.67494.e3.

Floerkemeier, T., Budde, S., Hurschler, C., Lewinski, G., Windhagen, H. and Gronewold, J. (2017), "Influence of size and CCD-angle of a short stem hip arthroplasty on strain patterns of the proximal femur an experimental study", *Acta Bioeng. Biomech.*, **19**(1), 141-149. https://doi.org/10.5277/ABB-00598-2016-02.

Fottner, A., Schmid, M., Birkenmaier, C., Mazoochian, F., Plitz,W. and Jansson, V. (2009), "Biomechanical evaluation of two types of short-stemmed hip prostheses compared to the trust plate prosthesis by three-dimensional measurement of micromotions", *Clinical Biomech.*, **24**(5), 429-434. https://doi.org/10.1016/j.clinbiomech.2009.02.007.

Gardner, M.P., Chong, A.C.M., Pollock, A.G. and Wooley, P.H. (2010), "Mechanical evaluation of large-size fourth-generation composite femur and tibia models", *Annal. Biomed. Eng.*, **38**, 613-620. https://doi.org/10.1007/s10439-009-9887-7.

Griffiths, S.Z., Post, Z.D., Buxbaum, E.J., Paziuk, T.M., Orozco, F.R., Ong, A.C. and Ponzio, D.Y. (2020), "Predictors of perioperative vancouver b periprosthetic femoral fractures associated with the direct anterior approach to total hip arthroplasty", *J. Arthroplasty*, **35**(5), 1407-1411. https://doi.org/10.1016/j.arth.2019.12.009.

Hajmohammad, M.H., Farrokhian, A. and Kolahchi, R. (2021), "Dynamic analysis in beam element of wave-piercing Catamarans undergoing slamming load based on mathematical modelling", *Ocean Eng.*, **234**, 109269. https://doi.org/10.1016/j.oceaneng.2021.109269.

Hambli, R. (2014), "3D finite element simulation of human proximal femoral fracture under quasi-static load", *Biomater. Biomec. Bioeng.*, **1**(4), 175-188. http://doi.org/10.12989/bme.2014.1.4.175.

Haversath, M., Lichetzki, M., Serong, S., Busch, A., Landgraeber, S., Jäger, M. and Tassemeier, T. (2020), "The direct anterior approach provokes varus stem alignment when using a collarless straight tapered stem", *Archiv. Orthopaedic Trauma Surg.*, **141**, 891-897. https://doi.org/10.1007/s00402-020-03457-9.

Huang, X., Hao, H., Oslub, K. Habibi, M. and Tounsi, A. (2021), "Dynamic stability/instability simulation of the rotary size-dependent functionally graded microsystem.", *Eng. Comput.*, https://doi.org/10.1007/s00366-021-01399-3.

Kalaiyarasan, A., Sankarb, K. and Sundarama, S. (2020), "Finite element analysis and modeling of fractured femur bone", *Mater. Today Proc.*, **22**(3), 649-653. https://doi.org/10.1016/j.matpr.2019.09.036.

Keshtegar, B., Nehdi, M.L., Trung, N-T. and Kolahchi, R. (2021), "Predicting load capacity of shear walls using SVR-RSM model", *Appl. Soft Comput.*, **112**, 107739. https://doi.org/10.1016/j.asoc.2021.107739.

Keshtegar, B., Xiao, M., Kolahchi, R. and Trung, N.T. (2020), "Reliability analysis of stiffened aircraft panels

using adjusting mean value method", *AIAA J.*, **58**(12). https://doi.org/10.2514/1.J059636.

Kolahchi, R., Keshtegar, B. and Trung, N.T. (2021), "Optimization of dynamic properties for laminated multiphase nanocomposite sandwich conical shell in thermal and magnetic conditions", *J. Sandw. Struct. Mater.*, **24**(1), 643-662. https://doi.org/10.1177/10996362211020388.

Kolahchi, R. and Kolahdouzan, F. (2021), "A numerical method for magneto-hygro-thermal dynamic stability analysis of defective quadrilateral graphene sheets using higher order nonlocal strain gradient theory with different movable boundary conditions", *Appl. Math. Model.*, **91**, 458-475. https://doi.org/10.1016/j.apm.2020.09.060.

Kolahchi, R., Tian, K., Keshtegar, B., Li, Z., Trung, N.T. and Thai, D-K. (2020), "AK-GWO: A novel hybrid optimization method for accurate optimum hierarchical stiffened shells", *Eng. Comput.*, 1-13. https://doi.org/10.1007/s00366-020-01124-6.

Kumar, K.C.N., Tandon, T., Silori, P. and Shaikh, A. (2015), "Biomechanical stress analysis of a human femur bone using ANSYS", *Mater. Today Proc.*, **2**(4-5), 2115-2120. https://doi.org/10.1016/j.matpr.2015.07.211.

Li, S., Abdel-Wahab, A., Demirci, E. and Silberschmidt, V.V. (2014), "Fracture process in cortical bone: X-FEM analysis of microstructured models", *Fract. Phen. Nat. Tech.*, 43-55. https://doi.org/10.1007/978-3-319-04397-5_5.

Michalski, A.S., Edwards, W.B. and Boyd, S.K. (2017), "The influence of reconstruction kernel on bone mineral and strength estimates using quantitative computed tomography and finite element analysis", *J. Clinical Densitometry*, **22**(2), 219-228. https://doi.org/10.1016/j.jocd.2017.09.001.

Mobasseri, S., Sadeghi, M., Janghorban, M. and Tounsi A. (2020), "Approximated 3D non-homogeneous model for the buckling and vibration analysis of femur bone with femoral defects", *Biomater. Biomec. Bioeng.*, **5**(1), 25-35. https://doi.org/10.12989/bme.2020.5.1.025.

Motezaker, M., Kolahchi, R., Rajak, D.K. and Mahmoud, S.R. (2021), "Influences of fiber reinforced polymer layer on the dynamic deflection of concrete pipes containing nanoparticle subjected to earthquake load", *Polym. Compos.*, **42**(8), 4073-4081. https://doi.org/10.1002/pc.26118.

Nişanci, G.N., Güvercin, Y., Ateş, S.M., Ölmez, H., Yaylacı E.U. and Yaylacı, M. (2020), "Investigation of the effect of different prosthesis designs and numbers on stress, strain and deformation distribution", *Int. J. Appl. Sci. Eng.*, **12**(4), 138-152. https://doi.org/10.24107/ijeas.816227.

Parashar, S.K. and Sharma, J.K. (2016), "A review on application of finite element modelling in bone biomechanics", *Perspect. Sci.*, **8**, 696-698. https://doi.org/10.1016/j.pisc.2016.06.062.

Pastrava, L.C., Devosa, J., Van Der Perrea, G. and Jaecquesa, S.V.N. (2009), "A finite element analysis of the vibrational behaviour of the intra-operatively manufactured prosthesis-femur system", *Med. Eng. Phys.*, **31**(4), 489-494. https://doi.org/10.1016/j.medengphy.2008.11.017.

Peitgen, D.S., Innmann, M.M., Merle, C., Gotterbarm, T., Moradi, B. and Streit, M.R. (2019), "Cumulative long-term incidence of postoperative periprosthetic femoral fractures using an uncemented tapered titanium hip stem: 26- to 32-year results", *J. Arthroplasty*, **34**(1), 77-81. https://doi.org/10.1016/j.arth.2018.08.038.

Peleg, E., Mosheiff, R., Liebergall, M. and Mattan, Y.A. (2006), "Short plate compression screw with diagonal bolts-a biomechanical evaluation performed experimentally and by numerical computation", *Clinical Biomech.*, **21**(9), 963-968. https://doi.org/10.1016/j.clinbiomech.2006.06.001.

Ramakrishna, S. and Pavani, B. (2020), "Design and stress analysis of femur bone implant with composite plates", *Biomater. Biomec. Bioeng*, **5**(1), 37-50. https://doi.org/10.12989/bme.2020.5.1.037.

Reimeringer, M. and Nuno, N. (2016), "The influence of contact ratio and its location on the primary stability of cementless total hip arthroplasty, A finite element analysis", *J. Biomech.*, **49**(7), 1064-1070. https://doi.org/10.1016/j.jbiomech.2016.02.031.

Schmidutz, F., Woiczinski, M., Kistler, M., Schröder, C., Jansson, V. and Fottner, A. (2017), "Influence of different sizes of composite femora on the biomechanical behavior of cementless hip prosthesis", *Clinical Biomech.*, **41**, 60-65. https://doi.org/10.1016/j.clinbiomech.2016.12.003.

Shariati, A., Ghabussi, A., Habibi, M., Safarpour, H., Safarpour, M., Tounsi, A. and Safa, M. (2020), "Extremely large oscillation and nonlinear frequency of a multi-scale hybrid disk resting on nonlinear elastic foundation", *Thin Wall. Struct.*, **154**, 106840. https://doi.org/10.1016/j.tws.2020.106840.

Shariati, A., Habibi, M., Tounsi, A., Safarpour, H. and Safa, M. (2021), "Application of exact continuum size-

dependent theory for stability and frequency analysis of a curved cantilevered microtubule by considering viscoelastic properties", *Eng. Comput.*, **37**, 3629-3648. https://doi.org/10.1007/s00366-020-01024-9.

Shishido, T., Tateiwa, T., Takahashi, Y., Masaoka, T., Ishida, T. and Yamamoto, K. (2018), "Effect of stem alignment on long-term outcomes of total hip arthroplasty with cementless Bi-Metric femoral components", *J. Orthopaedics*, **15**(1), 134-137. https://doi.org/10.1016/j.jor.2018.01.008.

Solidworks 2018, (2018), Dassault Systèmes Solidworks Corporation. Waltham MA, USA.

Streit, M.R., Merle, C., Clarius, M. and Aldinger, P.R. (2011), "Late peri-prosthetic femoral fracture as a major mode of failure in uncemented primary hip replacement", *J. Bone Joint Surg. Br.*, **93**(2), 178-183. https://doi.org/10.1302/0301-620X.93B2.24329.

Taherifar, R., Zareei, S.A., Bidgoli, M.R. and Kolahchi R. (2021), "Application of differential quadrature and Newmark methods for dynamic response in pad concrete foundation covered by piezoelectric layer", *J. Comput. Appl. Math.*, **382**, 113075. https://doi.org/10.1016/j.cam.2020.113075.

Talip, Ç. and Kişioğlu, Y. (2019), "Evaluation of new hip prosthesis design with finite element analysis", *Australas. Phys. Eng. Sci.*, **42**, 1033-1038. https://doi.org/10.1007/s13246-019-00802-0.

Terzi, M., Güvercin, Y., Ateş, S.M., Sekban, D.M. and Yaylacı, M. (2020), "Effect of different abutment materials on stress distrıbution in peripheral bone and dental implant system", *Sigma J. Eng. Nat. Sci.*, **38**(3), 1495-1507.

Tomlin, A., Sanders, M.B. and Kingsley, K. (2016), "The effects of cryopreservation on human dental pulp-derived mesenchymal stem cells", *Biomater. Biomec. Bioeng*, **3**(2), 105-114. http://doi.org/10.12989/bme.2016.3.2.105.

Tu, Y.K., Liu, Y.Ç., Yang, W.J., Chen, L.W., Hong, Y.Y., Chen, Y.C. and Lin, L.C. (2009), "Temperature rise simulation during a kirschner pin drilling in bone", *Bioinformatics and Biomedical Engineering ICBBE 2009 3rd International Conference on Beijing*, 1-4. https://doi.org/10.1109/ICBBE.2009.5163563.

Wadatkar, N.D., Londhe, S.D. and Metkar, R.M. (2020), "Stress analysis of fractured femur bone and implant of different metallic biomaterials", *Trends Biomater. Artif. Organs*, **34**(3), 96-99.

Wang, G., Huang, W., Song, Q. and Liang, J. (2017), "Three-dimensional finite analysis of acetabular contact pressure and contact area during normal walking", *Asian J. Surg.*, **40**(6), 463-469. https://doi.org/10.1016/j.asjsur.2016.07.002.

Watanabe, Y., Shiba, N., Matsuo, S., Higuchi, F., Tagawa, Y. and Inoue, A. (2000), "Biomechanical study of the resurfacing hip arthroplasty: Finite element analysis of the femoral component", *J. Arthroplasty*, **15**(4), 505-511. https://doi.org/10.1054/arth.2000.1359.

Yan, S.G., Chevalier, Y., Liu, F., Hua, X., Schreiner, A., Jansson, V. and Schmidutz, F. (2020), "Metaphyseal anchoring short stem hip arthroplasty provides a more physiological load transfer: A comparative finite element analysis study", *J. Orthopaedics Surg. Res.*, **15**, 1-10. https://doi.org/10.1186/s13018-020-02027-4.

Yan, S.G., Weber, P., Steinbruck, A., Hua, X., Jansson, V. and Schmidutz, F. (2018), "Periprosthetic bone remodelling of short-stem total hip arthroplasty: A systematic review", *Int. Orthopaedics*, **42**(9), 2077-2086. https://doi.org/10.1007/s00264-017-3691-z.

Zang, J., Uchiyama, K., Moriya, M., Li, Z., Fukushima, K., Yamamoto, T., Takahira, N., Takaso M., Liu J. and Feng, W. (2018), "Long-term clinical and radiographic results of the cementless Spotorno stem in Japanese patients: A more than 15-year follow-up", *J. Orthopaedics Surg.*, **26**(1), 1-7. https://doi.org/10.1177/2309499017750310.

CC